

Photo-oxidative tuning of individual and coupled GaAs photonic crystal cavities

Alexander Y. Piggott,^{1, a)} Konstantinos G. Lagoudakis,¹ Tomas Sarmiento,¹ Michal Bajcsy,^{1, 2} Gary Shambat,¹ and Jelena Vučković¹

¹⁾ *E. L. Ginzton Laboratory, Stanford University, California, USA*

²⁾ *Institute for Quantum Computing, University of Waterloo, Ontario, Canada*

(Dated: 31 January 2014)

We demonstrate a new photo-induced oxidation technique for tuning GaAs photonic crystal cavities using a 390 nm pulsed laser with an average power of 10 μ W. The laser oxidizes a small (~ 500 nm) diameter spot, reducing the local index of refraction and blueshifting the cavity. The tuning progress can be actively monitored in real time. We also demonstrate tuning an individual cavity within a pair of proximity-coupled cavities, showing that this method can be used to correct undesired frequency shifts caused by fabrication imperfections in cavity arrays.

Photonic crystal cavities have received significant attention in recent years for their ability to strongly confine light with high quality factors¹. These unique attributes have enabled them to be used in extensive studies of cavity quantum-electrodynamics (QED)^{2–4}, and for the implementation of a variety of compact classical devices such as low-power lasers⁵, high-speed light-emitting diodes⁶, and nonlinear frequency conversion devices⁷. Many of these devices are fabricated using GaAs since thin membranes with embedded quantum dots or quantum wells can be grown epitaxially.

A number of exciting devices using coupled photonic crystal cavities have been proposed and demonstrated. In the cavity QED domain, a wide range of proposals using coupled photonic crystal cavities have been put forward, including sub-poissonian light generation^{8–10}, the quantum simulation of exotic many-body systems¹¹, and quantum error correction¹². Coupled resonant oscillator waveguides (CROWs) can be constructed using a linear array of photonic crystal cavities¹³. Coupled cavity array lasers have also been demonstrated¹⁴.

Coupled cavity devices require the cavity resonances to be spectrally aligned with each other. In addition, cavity QED devices generally require the cavity resonances to be aligned with the emitter. Due to fabrication imperfections, the resonant wavelength of identically designed photonic crystal cavities typically varies by several nanometers, even for devices only a few microns apart. Thus, there has been considerable interest in the post-fabrication tuning of photonic crystal cavities.

A number of techniques for post-fabrication tuning of GaAs photonic crystal cavities have been demonstrated. These include wet etching¹⁵, infiltration of water^{16,17}, deposition of photosensitive materials^{18,19}, thermal oxidation²⁰, atomic-force microscope (AFM) oxidation²¹, green laser photo-oxidation²², and application of strain to the entire chip²³. However, many of these techniques are not well localized and hence cannot

be used to tune individual cavities in coupled cavity configurations, while others require the application of fluids or polymers, or the use of an AFM.

We describe a new, more convenient technique for tuning GaAs photonic crystal cavities using 390 nm pulsed laser light to introduce photo-induced oxidation. The laser oxidizes a small (~ 500 nm) diameter spot, lowering the local index of refraction and blueshifting the cavity. Our approach exploits the same physical mechanism as Intonti et al.²², which utilized a 532 nm laser at a relatively high power (700 μ W). By using a shorter-wavelength laser, we were able to reduce the tuning power by nearly 2 orders of magnitude while maintaining similar tuning rates, potentially enabling tuning of fragile structures such as nanobeam cavities²⁴. Finally, to demonstrate the resolution and utility of our approach, we demonstrate tuning individual cavities in proximity-coupled pairs of cavities.

The photonic crystal cavities used in this experiment were L3 cavities in a triangular photonic crystal lattice¹, with lattice constant $a = 336$ nm and design hole radius $r = 0.212a$. The fundamental mode for the L3 cavity calculated using finite-difference time-domain (FDTD) simulations is plotted in figure 1a, and has a simulated quality factor of $\sim 4 \times 10^4$. We tested the proposed tuning mechanism on both individual cavities and pairs of proximity-coupled cavities. The coupled L3 defects were placed 5 lattice periods apart, with a spectral splitting of 1.2 nm calculated using FDTD. Scanning electron microscopy (SEM) images of these structures are shown in figure 1c and figure 1d.

The photonic crystal cavities were fabricated from GaAs wafers grown using molecular beam epitaxy, as described in previous works⁵. The material stack consisted of a 220 nm GaAs membrane and a 1500 nm $\text{Al}_{0.8}\text{Ga}_{0.2}\text{As}$ sacrificial layer on top of a GaAs substrate. The GaAs membrane contained 3 layers of high-density InAs quantum dots (300 dots/ μm^2) emitting at wavelengths near 1300 nm. The photonic crystal cavities were fabricated using electron-beam lithography, inductively-coupled plasma reactive-ion etching (ICP-RIE), and a final HF acid undercutting step, as described previously⁴.

^{a)} Electronic mail: piggott@stanford.edu

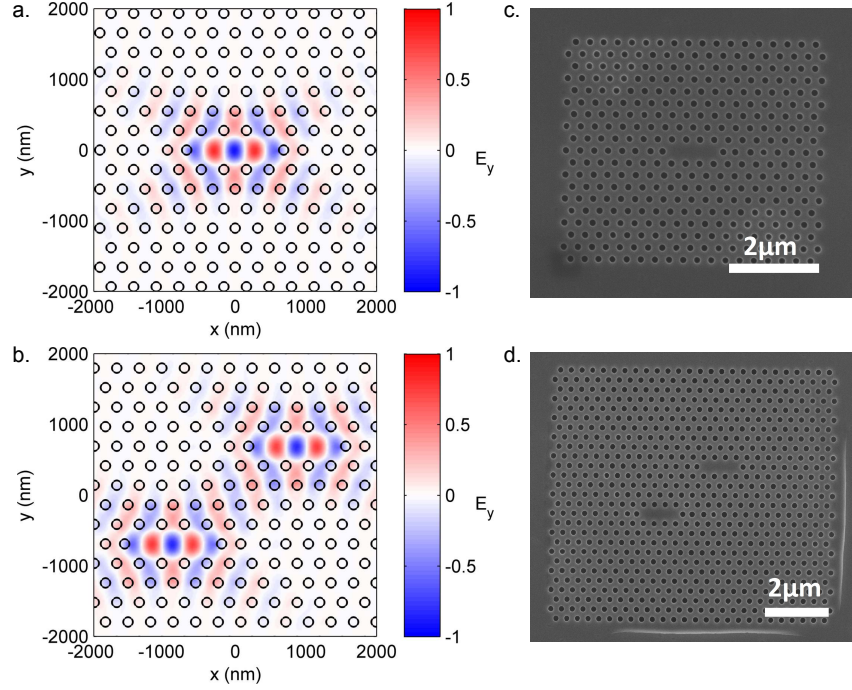


FIG. 1. (a,b) The transverse electric field (E_y) distribution for the fundamental modes of a (a) single L3 cavity and (b) two coupled L3 cavities, calculated in a finite-difference time domain (FDTD) simulation. The coupled cavity supports both anti-symmetric and symmetric modes; here we have plotted the latter. The black circles indicate the locations of the holes in the photonic crystal membrane. (c,d) Scanning electron microscopy (SEM) images of a single (c) and coupled (d) GaAs L3 cavities, taken before performing any tuning.

The tuning was performed in a custom confocal microscopy setup coupled to a grating spectrometer with an InGaAs ($1.7\ \mu\text{m}$) linear photodiode array. A Carl Zeiss LD-Plan-Neofluar 63x/0.75 Korr was used as the microscope objective. A charge-coupled device (CCD) integrated into the microscopy setup was used to both image the sample, and determine where the lasers were focused. The experiments were all performed at room temperature in air, with the exception of an additional control test where the sample was placed in vacuum.

The photonic crystal cavities were tuned by simultaneously irradiating the sample with two lasers through the objective: the 390 nm ultraviolet (UV) tuning laser, and an 830 nm near-infrared pump laser to produce photoluminescence (PL) from the quantum dots embedded in the photonic crystal membranes.

For the tuning laser, we used a frequency-doubled pulsed Ti:Sapphire laser, producing an output wavelength of 390 nm, pulse repetition frequency of 80 MHz, and an average power of $10\ \mu\text{W}$ before the microscope objective. The pulse length was approximately 10 ps after passing through a single-mode fiber (SMF) to clean up the beam profile. The UV laser was focused either directly on or immediately adjacent to the cavity to be tuned. The spot size of the tuning laser was roughly $500 - 700\ \text{nm}$ as estimated from SEMs of tuned devices.

An 830 nm, $350\ \mu\text{W}$ SMF-coupled continuous-wave multimode diode laser was used as the PL excitation

laser. The PL laser was somewhat defocused in order to tightly focus the UV tuning laser, so it was necessary to use a relatively high power to produce a bright PL signal. Due to the Purcell effect, the spontaneous emission rate from a photonic crystal cavity is strongly enhanced at its resonant frequencies²⁵. The photoluminescence spectrum was thus used to continuously monitor the cavity resonance during the tuning process. In principle, cross-polarized reflectivity measurements could also be used to monitor the cavity resonance when tuning non-photoluminescent devices⁴.

In figure 2a, we present the tuning profile of a single L3 cavity. The tuning rate decreases as a function of time, suggesting a self-limiting mechanism. The tuning rate can be increased by increasing the UV laser power, but using excessively high power risks damaging the membrane due to thermal effects. The initial and final spectra are plotted in figure 2b. The cavity quality factor (Q) is somewhat degraded by the tuning process, being reduced from $Q_{\text{initial}} = 4360$ to $Q_{\text{final}} = 2300$.

Next, in figures 2c and 2d we present the tuning of a single cavity in a proximity-coupled pair of L3 cavities. The behaviour of such a system can be accurately described using coupled-mode theory²⁶. Due to the coupling between the cavities, such a system will present two resonant peaks with frequencies Ω_1, Ω_2 given by

$$\Omega_{1,2} = \frac{1}{2}(\omega_1 + \omega_2) \pm \frac{1}{2}\sqrt{(\omega_1 - \omega_2)^2 + J^2} \quad (1)$$

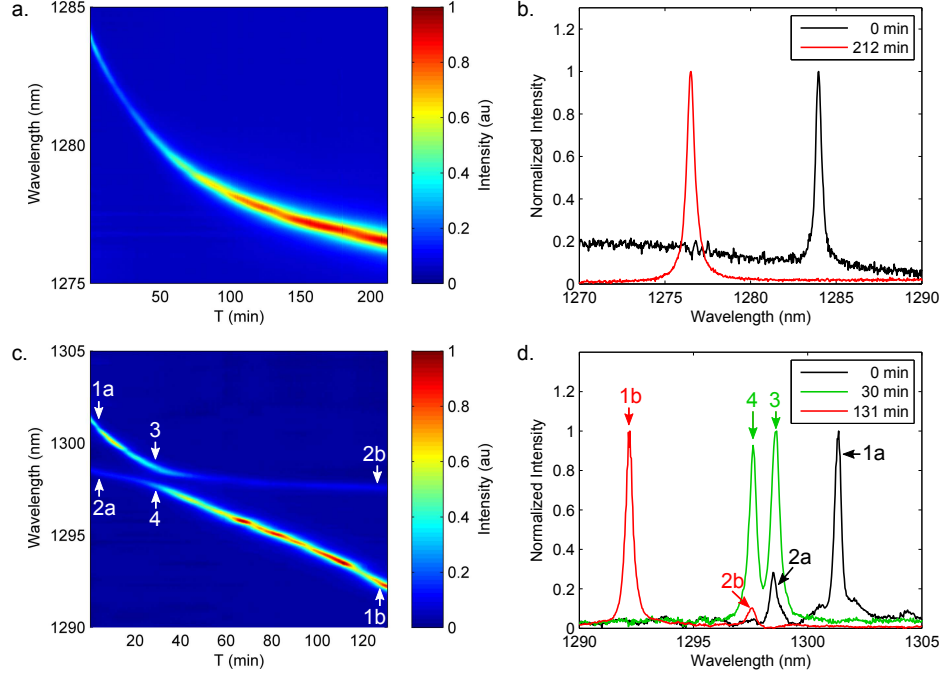


FIG. 2. Photoluminescence spectrum of (a,b) a single L3 cavity and (c,d) coupled L3 cavities as a function of time while tuning with the 390 nm UV laser. Due to Purcell enhancement, the cavity resonances are clearly visible. We have performed background subtraction for clarity. (a) The single cavity was blueshifted by 7.8 nm during the tuning process. (b) Initial and final photoluminescence spectra for the same cavity. The cavity quality factor was somewhat degraded by the tuning process, being reduced from $Q_{initial} = 4360$ to $Q_{final} = 2300$. (c) In the coupled-cavity system, one cavity was tuned by 9.1 nm, and the other cavity was tuned by only 1.0 nm, resulting in a clear anti-crossing where their resonances became degenerate. (d) Initial, intermediate (during the anticrossing), and final spectra for the coupled cavity system. The microscope was focused on the tuned cavity, resulting in a brighter PL signal from the tuned cavity than the untuned cavity.

where ω_1, ω_2 are the individual cavity frequencies, and J is the coupling between the cavities. We have assumed the cavities are in the strong coupling limit $J \gg \omega_i/Q_i$, where the Q_i is the quality factor of cavity i .

The UV laser was focused on one edge of a cavity, as can be seen in an SEM of the tuned structure in figure 3a. As the UV laser was applied, the resonant peak at 1298.5 nm remained nearly stationary while the other resonant peak blueshifted from 1301.3 nm to 1292.2 nm. As the two peaks pass each other, a clear anti-crossing - which arises from equation (1) - can be observed.

The tuning mechanism is likely photo-induced oxidation of GaAs by the 390 nm UV laser, resulting in reduction of the local index of refraction and blueshifting the cavities. Previous research has shown that photo-oxidation of GaAs surfaces can be induced by UV irradiation under similar parameters to our experiment²⁷⁻²⁹. SEMs of tuned cavities are shown in figure 3. No damage to the photonic crystal is visible other than a slight discoloration and reduction in hole size in the vicinity of the irradiated spot, probably due to the growth of oxide on the surface. We also conducted identical experiments in a vacuum chamber pumped down to $\sim 10^{-4}$ Torr, and there was no observable tuning or change in appearance.

Due to the low power of our UV tuning laser, the tuning mechanism is very unlikely to be thermal oxidation.

The steady state temperature increase should be very small. Based on Sentaurus simulations of similar structures, we expect to see a temperature rise of < 1 K for a heat dissipation of $10 \mu\text{W}$ ³⁰. We also see no permanent tuning effects from our higher power $350 \mu\text{W}$ PL laser.

The instantaneous temperature rise from each UV laser pulse is expected to be much higher, but still relatively low. Assuming a plane wave propagating into an infinite slab of GaAs, and ignoring reflections, the local temperature rise ΔT from a single pulse is given by

$$\Delta T = \Phi_0 \frac{\alpha e^{-\alpha z}}{\rho C} \quad (2)$$

where Φ_0 is the incident fluence (W/cm^2), $\alpha = 7.433 \times 10^5 \text{ 1/cm}$ is the extinction coefficient of GaAs at 390 nm³¹, $C = 0.350 \text{ J/g K}$ and $\rho = 5.320 \text{ g/cm}^3$ are the heat capacity and density of GaAs³², and z is the distance from the incident surface. If we assume the incident light is a gaussian beam with a diameter of 500 nm, the estimated temperature rise at the surface ($z = 0$) is 50.8 K, far too low for thermally-induced oxidation. Since we assumed there are no reflections, and used a conservative estimate of laser spot size based on our SEMs, this should be an overestimate of the actual temperature rise.

In conclusion, we have demonstrated a technique for

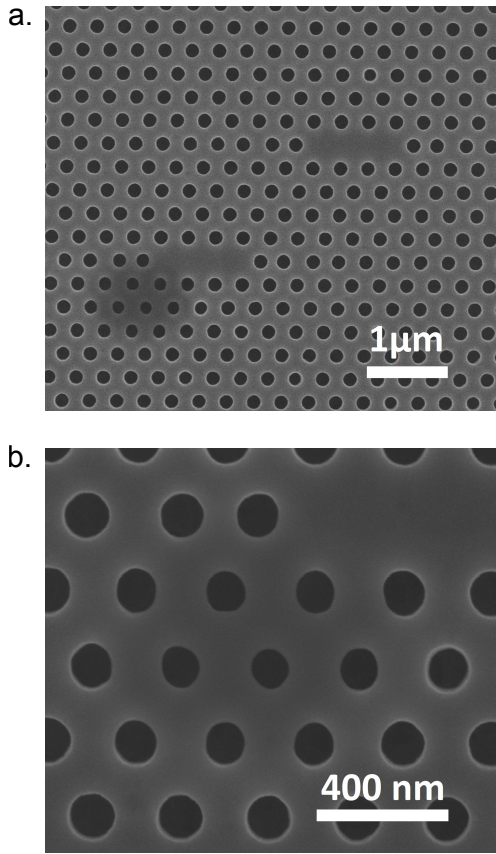


FIG. 3. Scanning electron microscopy (SEM) image of a coupled L3 system after performing tuning, showing (a) the entire structure and (b) zoomed in on the laser oxidized spot. The oxidation is visible as a slight discoloration, and the photonic crystal holes are also reduced in size due to the growth of oxide on the surface.

tuning GaAs nanophotonic resonators which requires only a low-power UV laser at room temperature in ambient atmosphere. In particular, this technique can be used to independently tune individual cavities in proximity-coupled cavity configurations, allowing the fabrication of a wide range of coupled-cavity devices with applications ranging from quantum simulations and information processing to low-power nanophotonic lasers.

ACKNOWLEDGMENTS

The authors acknowledge support provided by the Air Force Office of Scientific Research (AFOSR) MURI Center for Multi-Functional Light-Matter Interfaces based on Atoms and Solids (FA9550-09-1-0704), and the AFOSR MURI for Complex and Robust On-chip Nanophotonics (FA9550-12-1-0025). AYP acknowledges support from the Stanford Graduate Fellowship. KGL acknowledges support from the Swiss National Science Foundation.

¹Y. Akahane, T. Asano, B.-S. Song, and S. Noda, *Nature* **425**, 944 (2003).

- ²J. Vučković, M. Lončar, H. Mabuchi, and A. Scherer, *Phys. Rev. E: Stat., Nonlinear, Soft Matter Phys.* **65**, 016608 (2001).
- ³T. Yoshie, A. Scherer, J. Hendrickson, G. Khitrova, H. M. Gibbs, G. Rupper, C. Ell, O. B. Shchekin, and D. G. Deppe, *Nature* **432**, 200 (2004).
- ⁴D. Englund, A. Faraon, I. Fushman, N. Stoltz, P. Petroff, and J. Vučković, *Nature* **450**, 857 (2007).
- ⁵B. Ellis, M. A. Mayer, G. Shambat, T. Sarmiento, J. Harris, E. E. Haller, and J. Vučković, *Nature Photonics* **5**, 297 (2011).
- ⁶G. Shambat, B. Ellis, A. Majumdar, J. Petykiewicz, M. A. Mayer, T. Sarmiento, J. Harris, E. E. Haller, and J. Vučković, *Nature Communications* **2**, 539 (2011).
- ⁷K. Rivoire, Z. Lin, F. Hatami, W. T. Masselink, and J. Vučković, *Optics Express* **17**, 22609 (2009).
- ⁸T. C. H. Liew and V. Savona, *Phys. Rev. Lett.* **104**, 183601 (2010).
- ⁹M. Bamba, A. Imamoğlu, I. Carusotto, and C. Ciuti, *Phys. Rev. A: At., Mol., Opt. Phys.* **83**, 021802 (2011).
- ¹⁰A. Majumdar, M. Bajcsy, A. Rundquist, and J. Vučković, *Phys. Rev. Lett.* **108**, 183601 (2012).
- ¹¹A. D. Greentree, C. Tahan, J. H. Cole, and L. C. L. Hollenberg, *Nature Physics* **2**, 856 (2006).
- ¹²J. Kerckhoff, H. I. Nurdin, D. S. Pavlichin, and H. Mabuchi, *Physical Review Letters* **105**, 040502 (2010).
- ¹³A. Yariv, Y. Xu, R. K. Lee, and A. Scherer, *Opt. Lett.* **24**, 711 (1999).
- ¹⁴H. Altug and J. Vučković, *Opt. Express* **13**, 8819 (2005).
- ¹⁵K. Hennessy, A. Badolato, A. Tamboli, P. M. Petroff, E. Hua, M. Atatüre, J. Dreiser, and A. Imamoğlu, *Appl. Phys. Lett.* **87**, 021108 (2005).
- ¹⁶N. W. L. Speijcken, M. A. Dndar, A. C. Bedoya, C. Monat, C. Grillet, P. Domachuk, R. Nötzel, B. J. Eggleton, and R. W. van der Heijden, *Appl. Phys. Lett.* **100**, 261107 (2012).
- ¹⁷S. Vignolini, F. Riboli, D. S. Wiersma, L. Balet, L. H. Li, M. Francardi, A. Gerardino, A. Fiore, M. Gurioli, and F. Intonti, *Appl. Phys. Lett.* **96**, 141114 (2010).
- ¹⁸T. Cai, R. Bose, G. S. Solomon, and E. Waks, *Appl. Phys. Lett.* **102**, 141118 (2013).
- ¹⁹A. Faraon, D. Englund, D. Bulla, B. Luther-Davies, Benjamin, J. Eggleton, N. Stoltz, P. Petroff, and J. Vučković, *Appl. Phys. Lett.* **92**, 043123 (2008).
- ²⁰H. S. Lee, S. Kiravittaya, S. Kumar, J. D. Plumhof, L. Balet, L. H. Li, M. Francardi, A. Gerardino, A. Fiore, A. Rastelli, and O. G. Schmidt, *Appl. Phys. Lett.* **95**, 191109 (2009).
- ²¹K. Hennessy, C. Högerle, E. Hu, A. Badolato, and A. Imamolou, *Appl. Phys. Lett.* **89**, 041118 (2006).
- ²²F. Intonti, N. Caselli, S. Vignolini, F. Riboli, S. Kumar, A. Rastelli, O. G. Schmidt, M. Francardi, A. Gerardino, L. Balet, L. H. Li, A. Fiore, and M. Gurioli, *Appl. Phys. Lett.* **100**, 033116 (2012).
- ²³I. J. Luxmoore, E. D. Ahmadi, B. J. Luxmoore, N. A. Wasley, A. I. Tartakovskii, M. Hugues, M. S. Skolnick, and A. M. Fox, *Appl. Phys. Lett.* **100**, 121116 (2012).
- ²⁴Y. Gong, B. Ellis, G. Shambat, T. Sarmiento, J. S. Harris, and J. Vučković, *Optics Express* **18**, 8781 (2010).
- ²⁵E. M. Purcell, *Phys. Rev.* **69**, 681 (1946).
- ²⁶H. A. Haus and W. Huang, *Proceedings of the IEEE* **79**, 1505 (1991).
- ²⁷C. Yu, D. Podlesnik, M. Schmidt, H. Gilgen, and R. O. Jr., *Chem. Phys. Lett.* **130**, 301 (1986).
- ²⁸C. F. Yu, M. T. Schmidt, D. V. Podlesnik, and R. M. Osgood, *J. Vac. Sci. Technol. B* **5**, 1087 (1987).
- ²⁹Z. Lu, M. T. Schmidt, D. V. Podlesnik, C. F. Yu, and R. M. Osgood, *J. Chem. Phys.* **93**, 7951 (1990).
- ³⁰J. Petykiewicz, G. Shambat, B. Ellis, and J. Vučković, *Applied Physics Letters* **101**, 011104 (2012).
- ³¹E. D. Palik, *Handbook of Optical Constants of Solids* (Elsevier Inc., 1997).
- ³²S. M. Sze, *Semiconductor Sensors* (John Wiley & Sons, 1994) p. 535.